JOURNAL OF MATERIALS SCIENCE 31 (1996) 3447–3451

Study of transition metal ion doped mullite by positron annihilation techniques

D. SANYAL, D. BANERJEE, R. BHATTACHARYA
Department of Physics, University of Calcutta, 92 Acharya Prafulla Chandra Road, Calcutta 700009, India

S. K. PATRA, S. P. CHAUDHURI
Central Glass and Ceramic Research Institute, Calcutta 700032, India

B. NANDI GANGULY, U. DE*
*Saha Institute of Nuclear Physics and * Variable Energy Cyclotron Centre, Department of Atomic Energy, 1/AF Bidhan Nagar, Calcutta 700064, India*

Mullite, an extremely useful ceramic material, is doped with transition metal ions. The changes in the electronic properties of these doped materials have been studied by positron annihilation lifetime spectroscopy as well as Doppler broadened line shape analysis. The results on the positron annihilation parameters are characteristic of ionic size, oxidation state and the "*d*"-electron configuration of the respective transition metals doped in the parent lattice of the mullite. These results, along with the resistivity measurements are suggestive of transition of the parent mullite from an insulator to a semimetal in the modified structure.

1. Introduction

Mullite, an aluminosilicate of normal composition, $3Al_2O_3 \cdot 2SiO_2$, is endowed with many excellent properties [1–3]. It has well established applications both in low and high temperature environments due to its low thermal expansion, high creep resistance and high mechanical strength. An important review work by Davis and Pask [4] incorporated the details of its thermodynamic, chemical, mechanical and electrical properties. In another review work Schneider [5, 6] dealt with its crystal structure, composition and the effect of incorporation of 3*d* transition metal ions at different oxidation states.

Mullite is built up of chains of aluminium oxygen octrahedra linked by double chains containing aluminium oxygen and silicon oxygen tetrahedra, in a random sequence [7, 8]. Some of these tetrahedral chains are misordered in such a manner that replacement of Si^{4+} ions by Al^{3+} ions occurs in the tetrahedra resulting in the removal of O^{2-} ions to preserve electroneutrality of the structure. This phenomenon introduces two oxygen vacancies in each unit cell of mullite rendering its structure more open for accommodating a host of cations, e.g. Mn^{2+}, Fe^{3+}, Cr^{3+}, Ti^{4+}, V^{4+}, Zr^{2+}, etc., as a substitutional or as an interstitial solid solution [9]. So, many non-stoichiometric mullite may be possible with Al_2O_3 in solid solution, and a change in electron density in the parent structure can be brought about by doping cations of different valency states. Both the oxygen vacancy defect and the effect of dopant cations are expected to cause a significant increase in the electrical conductivity of mullite at room temperature and particularly at elevated temperatures.

In the recent past some experimental knowledge on atomic defects and vacancy formation has been acquired in the case of metal oxides and ceramics through positron annihilation techniques [9]. In addition to this, yttria doping on ZrO_2, which is expected to generate oxygen vacancies, has been used as a test for the trapping capability of positrons at anion vacancies [10, 11]. Also, the annealing behaviour of electron irradiated Al_2O_3 has been studied to elucidate kinetic properties of the defects [12].

In the present work, the deviation of electronic and electrical properties of doped mullite from the parent mullite has been sensed by employing positron annihilation techniques and by electrical conductivity measurements. Positron annihilation lifetime spectroscopy (PALS), to probe the electronic environment as a function of doping concentration, and also Doppler broadened annihilation radiation lineshape analysis (DBARLA), to probe the possible change of electron momentum distribution as a function of the doping concentration, have been done. The electrical property has also been evaluated by conductivity measurements on the parent and doped mullite samples.

To substitute transition metal ions in the octahedra, ions with radii close to that of Al^{3+} and identical ionic charge are best suited. Ions with higher ionic charge, e.g. Ti^{4+}, or lower ionic charge, e.g. Mn^{2+}, are less favourable since in this situation simultaneous tetrahedral substitution of silicon by aluminium is required

0022–2461

TABLE I The ionic properties [8, 13, 14] of transition metals doped in mullite crystal, in comparison to Al^{3+} in the chains of Al–O octahedra

Metal ions	Electronic configuration	Size of the ions (nm)	Preferred site of incorporation
Fe^{3+}	$[Ar]3d^5 4s^0$	0.064	Octahedral Tetrahedral (in small amounts)
Cr^{3+}	$[Ar]3d^3 4s^0$	0.064	Octahedral
Mn^{2+}	$[Ar]3d^5 4s^0$	0.083	Octahedral
Ti^{4+}	$[Ar]3d^0 4s^0$	0.068	Octahedral
Al^{3+}	$[Ne]3s^0 3p^0$	0.052	Octahedral

to compensate for the excess positive charge. In the present studies Fe, Mn, Cr and Ti have been used as dopants in mullite. Table I shows their charge states and radii. From this table it can be seen that, of these four ions, Fe and Cr are more favourable compared to Mn and Ti ions.

2. Experimental procedure

2.1. Chemical preparation of the samples

An aqueous solution of analytical reagent (AR) grade $Al(NO_3)_3 \cdot 9H_2O$ and AR grade $Si(OC_2H_5)_4$ solution is mixed thoroughly in an ammoniacal medium (pH $\equiv$ 9.3) to coprecipitate hydroxides of Al and Si. Each of the four dopant ions is incorporated in four different concentrations by adding its water soluble salt into the medium during coprecipitation. After filtration and drying, the coprecipitate is calcined at 500 °C for 3 h. This reactive powder is then moistened with an organic binder and then pressed into discs which are finally sintered at 1600 °C for 3 h in an electric furnace within an oxidizing atmosphere. The discs (25 mm diameter × 5 mm height) are finally ground and polished.

The samples are checked by X-ray diffraction, X-ray fluorescence and wet chemical analyses for their purity and Al_2O_3:SiO_2 stoichiometry. The samples have been found to be 99.9% pure mullite having compositions of $3Al_2O_3 \cdot 2SiO_2$. The amount of dopant present in each of the doped samples is checked by X-ray fluorescence and wet chemical analysis.

2.2. Positron annihilation lifetime measurement

The source of positron (^{22}Na-4 μCi) is deposited on a thin Mylar film (400 μg cm^{-2}) and sealed using another identical Mylar film on top of it. This source is sandwiched in between the two discs of the specimen and placed between the two scintillation detectors. The positron lifetime distribution measurements have been done using a conventional arrangement with a time to amplitude converter and a multichannel analyser. Two tapered Pilot U scintillators (2.5 cm diameter × 2.5 cm height) coupled to two RCA 8850 photomultiplier tubes constitute the two counters. The fast pulses are processed in constant fraction discriminators before being fed to the time to amplitude converter. This arrangement has a prompt time resolution full width at half maximum (FWHM) of 240 ps for the prompt ^{60}Co γ-rays at the positron experimental window settings, with the upper 60% of the respective compton continuum of the 1.28 and 0.511 MeV γ-rays. A total of one million peak counts have been accumulated in each case.

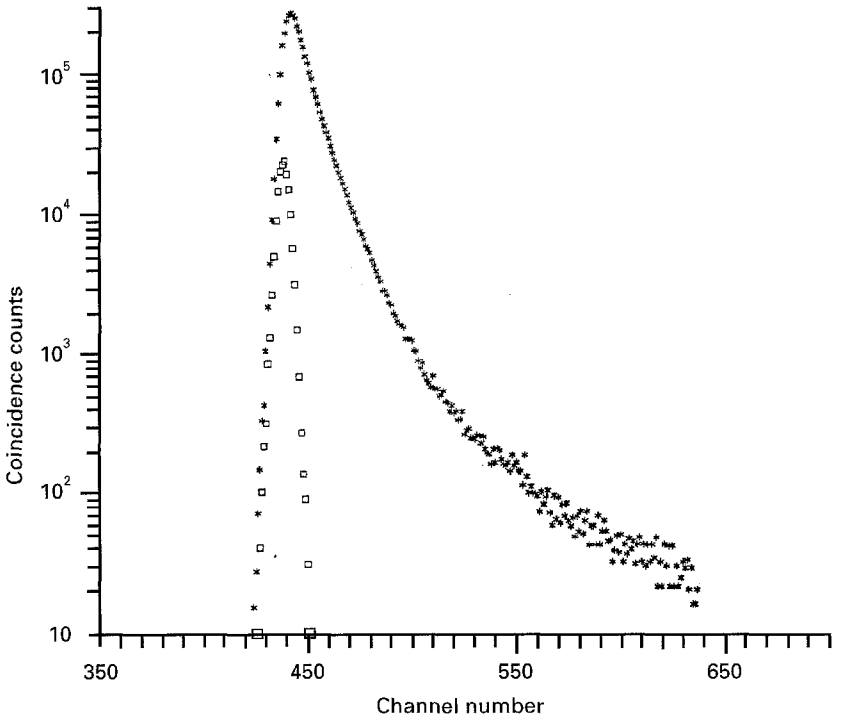

Figure 1 (*) A typical background subtracted positron lifetime spectrum for parent mullite; (□) the prompt curve giving FWHM ≡ 240 ps. Calibration: 40.00 ps per channel.

2.3. *S*-parameter measurement

The DBARLA study is done using a 40 cm^3 high purity Ge detector having a resolution (FWHM) of 1.12 keV at the 475 keV γ-ray from a ^{102}Rh source and of 1.16 keV at the 514 keV γ-ray from a ^{85}Sr source. A total of 10 million counts is accumulated in each case. Two sources (Ba-133 and Bi-207) have been used for energy calibration of the DBARLA system and the channel constant is set at 60 eV per channel. All the measurements have been done at the normal room temperature of 20 °C.

2.4. Data analysis

The data pertaining to the lifetime spectra are analysed with the help of the standard computer program PATFIT-88 [15]. The variance of fit in the analyses lay between 0.9 and 1.1. The line shape parameter, *S*, defined [16] as the sum of counts over a fixed number of channels around the centre of the annihilation peak divided by the peak area, is evaluated in connection with the DBARLA measurements. This parameter gives a measure of the narrowness of the annihilation line.

Typical lifetime and Doppler broadened annihilation spectra of doped mullite samples are shown in Figs 1 and 2, respectively.

2.5. Resistivity measurement

To measure the electrical resistivity, the samples are prepared in the form of discs. The discs are coated on both sides with Pt paste, dried and fired at 1000 °C for 15 min. A disc to be used in measurements is then placed in a Teflon sample holder inside a vacuum chamber electrically connected to ground. A very short coaxial cable is used to connect the sample to the electrometer input for minimizing electromagnetic and radio frequency interferences. A constant voltage (1.50 V) is applied and the current flowing through the sample is measured by the electrometer. Resistivity of the sample is then calculated.

3. Results and discussion

The positron lifetime spectrum recorded [17] in the mullite samples has been resolved into three different components

1. τ_1, characterized by a short lifetime which arises from the free residence positrons [12],

2. τ_2, a component with a somewhat longer lifetime which may be attributed to the partial trapping of positrons at residual extrinsic vacancy defects (impurity metal ion induced) or reduced electron density region in the crystal structure, and

3. an additional third component, τ_3, with long annihilation lifetime of ~2–3 ns with a very weak signature of average intensity of 2–3% which can be separated and ascribed to a pick-off component of the orthopositronium triplet [18].

The mean positron lifetime, $\bar{\tau}$, defined as $\bar{\tau} = \Sigma_i \tau_i I_i$ where I is the intensity, would be better suited here [17] to describe the change in the annihilation rate within the crystal (Fig. 3).

However, it is to be noted that the second longest lifetime component, τ_2, is the one which is most sensitive to the presence of the dopant element and its concentration. This component, therefore, can be associated with the trapping of the positrons by the lattice defect, or trapping in a region where the electronic charge density is fluctuating [18]. From the data (Fig. 4), it is evident that the annihilation rate increases as the "*d*" electron enters the system. Schaefer and Forster have [12] quantitatively correlated the annihilation rate of positrons with the electron densities of the materials. The same effect is corroborated from the present data, which shows that the annihilation rate increases as the dopant concentration increases; the associated intensity component also shows a similarly increasing trend. Morever, the annihilation properties are manifested here according to the number of "*d*" electrons of the dopant metal ions present, their ionic size and their respective capacity to be incorporated in the mullite structure [5, 6] (Table I).

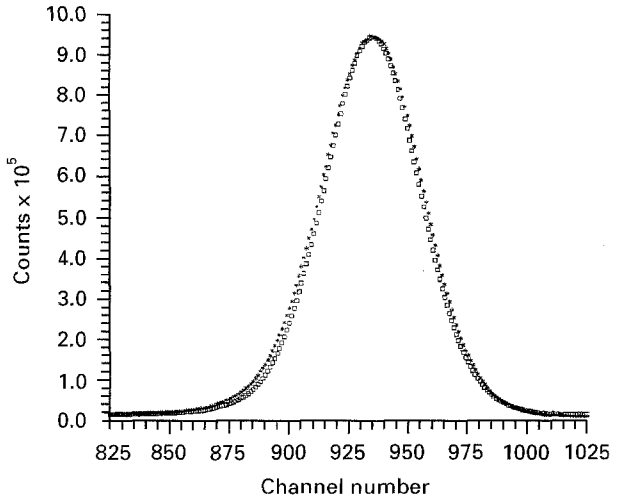

Figure 2 A typical Doppler broadened positron annihilation spectra from (□) parent mullite; (*) Fe^{3+} ion doped (1 wt %) mullite. Peak counts have been normalized. Calibration: 60 eV per channel.

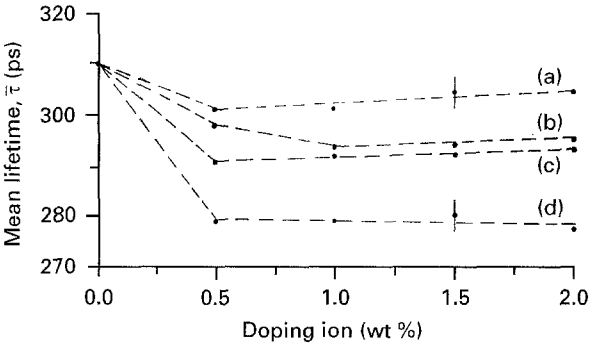

Figure 3 Variation of mean lifetime, $\bar{\tau}$, with concentration of different dopants in parent mullite. Curves labelled (a), (b), (c) and (d) are for dopants Mn^{2+}, Ti^{4+}, Fe^{3+} and Cr^{3+}, respectively. The few error bars shown indicate typical error in the measurement.

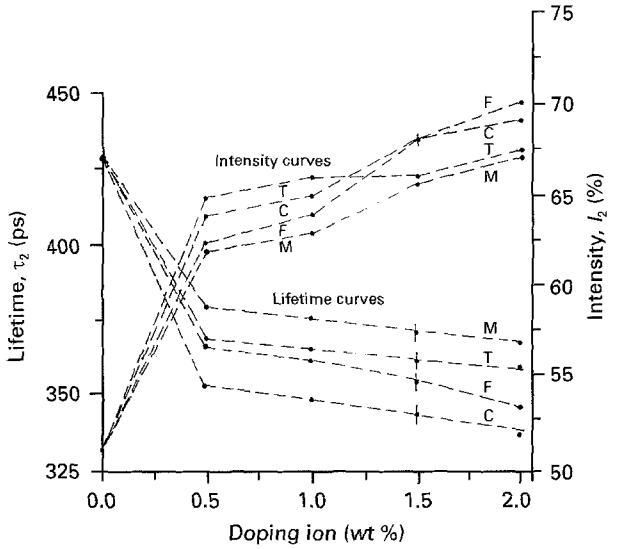

Figure 4 Variation of τ_2 and I_2 with concentration of different dopants in parent mullite. Curves labelled by M, F, C and T are for dopants Mn^{2+}, Fe^{3+}, Cr^{3+} and Ti^{4+}, respectively. The few error bars shown indicate typical error in the measurement.

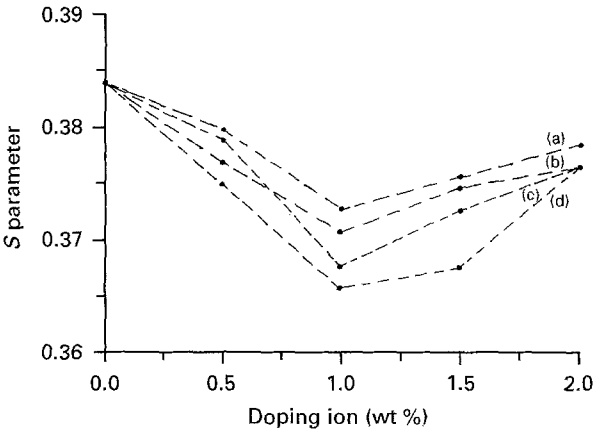

Figure 5 Variation of S parameter with concentration of different dopants in parent mullite. Curves labelled (a), (b), (c) and (d) are for dopants Mn^{2+}, Ti^{4+}, Cr^{3+} and Fe^{3+}, respectively. Errors, being very small (0.0005), have not been shown.

It turns out that the amount of transition metals in mullite is strongly dependent on the ionic radius and oxidation state of the cation. The highest incorporation is observed if the radius and oxidation state of a given cation correspond to those of Al^{3+}. The relatively large cation sizes and higher octahedral but lower tetrahedral crystal field splitting parameters of most transition metal ions oviate their preference for octahedral co-ordination [14]. Fe^{3+} and Mn^{2+} exhibit d^5 half filled stable electronic configuration with a spherically symmetric charge distribution, their incorporation being solely controlled by size distribution. In fact, highest incorporation is found for Fe^{3+} and Cr^{3+}. An extensive survey of the work on mullite [5,6] supports the existence of a small amount of Fe^{3+} in the oxygen tetrahedra at high temperature, in addition to its occupancy in the octahedral positions. The Cr^{3+} ions are distributed in the oxygen octahedra and in the interstitial lattice positions. In the present positron parameter results one finds a pronounced manifestation of the incorporation of these metals over the other two (Figs 4 and 5). The maximum amount of Ti^{4+} ions entering the mullite structure is about half of Cr^{3+} and Fe^{3+}. Only a small or a very small amount of Mn^{2+} ions enter into the mullite structure. The effect of this elemental ionic property is thus well exhibited by the positron annihilation parameters. In the parent mullite sample, the S parameter has a larger value compared to those in the doped ones; which means that the annihilation site corresponds, on average, to a low momentum region of the electrons. With the entry of the "d" electrons in the crystal lattice of the mullite, a decrease in S parameter starts; which reaches a minimum around 1% concentration in general, in case of the metal ions studied here and then rises again (Fig. 5). The nature of the curves is characteristic of the individual dopant metal ions studied in the present experiments.

The incorporation of 3d metal ions in the mullite crystal can be viewed upon as the localization of electrons which tends to increase the total kinetic energy of the system [19]. In transitional group elements, the interaction of ion cores with incomplete "d" electron shells are characterized by high binding energy [19]. All these effects may contribute to higher momentum transfer to the annihilation e^-e^+ pair and consequently the S parameter decreases [16], i.e. the narrow component fraction under the Doppler broadened annihilation curve decreases.

This gradual decrease in S parameter continues up to a concentration of $\simeq 1\%$ of the dopant element after which the 3d metal ion seems to make proper site specific interaction with the ionic core so as to stabilize the interatomic interaction within the crystal. The incorporated atoms in the crystal lattice must be bound in such a way that electrostatic attraction between the valence electrons and the ion cores ultimately attains an energetically stabilized configuration. In doing so, it may lower the potential energy of the system, but in such a way that the kinetic energy of the system does not increase much [19]. As a result, variation of the S parameters attains a shallow well shaped form, but the samples having metal incorporated still show lower values of S than that in the parent mullite sample. It is also to be noted that the manifestation of the positron, S parameters exactly match those of the valence states, ionic size and the individual property of the dopant elements [5, 6, 14].

In addition to this, the increase in positron annihilation rates [17] suggests that there is a transition of mullite from the insulator region to a semimetal region. Also the low S parameter values indicate the properties of the 3d valence shell or of the conduction electrons [16].

Comparison of the results of resistivity measurement (Table II) of the parent mullite sample with those of metal doped mullite samples shows a considerable decrease (about two orders) in resistivity. This effect again accounts for the incorporation of 3d transition metals in the periodic lattice of the mullite crystal structure which emerges with the

TABLE II Electrical resistivity of different mullite samples

Doped cation	Dopant concentration (wt %)	Resistivity (Ω cm)
Parent mullite	–	9.320×10^{12}
Mn^{2+}	0.5	1.055×10^{11}
	1.0	1.027×10^{11}
	1.5	1.172×10^{11}
	2.0	1.212×10^{11}
Fe^{3+}	0.5	1.550×10^{11}
	1.0	1.233×10^{11}
	1.5	1.289×10^{11}
	2.0	1.579×10^{11}
Cr^{3+}	0.5	1.325×10^{11}
	1.0	1.187×10^{11}
	1.5	1.661×10^{11}
	2.0	1.754×10^{11}
Ti^{4+}	0.5	1.820×10^{11}
	1.0	1.799×10^{11}
	1.5	1.876×10^{11}
	2.0	1.971×10^{11}

possibility of attaining a lower band gap structure [19]. This has a decisive significance in as much as it offers an explanation for the considerable lowering of resistivity at room temperature.

4. Conclusions

The positron annihilation results with the 3d transition metal ion doped mullite show much higher annihilation rates, unlike the parent mullite. The characteristics of the dopant elements, like ionic size, valence state, etc., are properly manifested in the annihilation parameters.

The S parameter results also exhibit the properties of the specific metal ions incorporated. The decrease in the values of the S parameters is indicative of transition of the doped mullite samples from an insulator to a semimetal. The resistivity measurement also bears a close correlation to this behaviour.

Acknowledgements

The authors express their gratitude to Professor P. Sen for his interest in the work. They are indebted to S. Kumar, S. Das and V. S. Subrahmanyam for helpful discussion. D. Sanyal thanks the University Grants Commission, Government of India for financial support. S. K. Patra is grateful to the Council of Scientific & Industrial Research, Government of India for granting financial assistance.

References

1. W. H. TAYLOR, *J. Soc. Glass Technol.* **16** (1932) 111.
2. J. R. ANGEL and C. T. PREWITT, *Amer. Min.* **71** (1986) 1476.
3. S. P. CHAUDHURI, *J. Can. Ceram. Soc.* **58** (1989) 61.
4. R. F. DAVIS and J. A. PASK, in "Refractory Materials, High Temperature Oxides, Part IV, Refractory Glasses, Glass-Ceramics and Ceramics," edited by A. M. Alper (Academic Press, New York, 1971) p. 37.
5. H. SCHNEIDER, in "Ceramic Transaction," Vol. 6, edited by S. Somiya, R. F. Davis and J. A. Pask (American Ceramic Society, OH, 1990) p. 135.
6. *Idem.*, Habiliationsschrift, University of Munster (1986) p. 1.
7. H. SCHNEIDER and H. RAGER, *J. Amer. Ceram. Soc.* **67** (1984) C 248.
8. J. C. BAILAR, H. J. EMELEUS, R. NYHOLM and A. F. TROTMAN-DICKSON (editors) "Comprehensive Inorganic Chemistry" Vol. 3 (Pergamon Press, Oxford, 1973) Ch. 32, 34, 36, 37 and 40.
9. M. FORSTER, W. CLAUDY, H. HERMES, M. KOH, K. MAIER, J. MAJOR, H. STALL and H. E. SCHAEFER, *Mater. Sci. Forum* **105** (1992) 1005.
10. J. F. BAUMARD and P. ABELARD in "Advances in Ceramics", Vol. 12, edited by N. Claussen, M. Rühle and A. Heuer (The American Ceramic Society, OH, 1983) p. 555.
11. KOFSTADT, "Nonstoichiometry, Diffusion and Electrical Conductivity in Binary Metal Oxdies" (Wiley-Interscience, New York, 1972).
12. H.-E. SCHAEFER and M. FORSTER, *Mater. Sci. Engng.* **A109** (1989) 161.
13. J. D. LEE, "A New Concise Inorganic Chemistry" (Van Nostrand & Reinhold, London, 1977) Ch. 5 and 6.
14. F. A. COTTON and G. WILKENSON, "Advanced Inorganic Chemistry: A Comprehensive Textbook", 5th Edn (Wiley, New Delhi, 1988) Ch. 18 and Appendix 4.
15. P. KIRKEGAARD, N. J. PEDERSEN and M. ELDROUP, Report of Riso National Lab Riso-M-2740 (1989).
16. J. J. KELLY and R. M. LAMBRECHT, in "Positronium and Muonium Chemistry", edited by H. J. Ache (American Chemical Society, Washington, DC, 1979) p. 271.
17. H. E. SCHAEFER, *Phys. Status Solidi (a)* **102** (1987) 47.
18. J. T. WABER, C. L. SNEAD Jr and K. G. LYNN, in "Positron Annihilation", edited by P. C. Jain, R. M. Singru and K. P. Gopinathan (World Scientific, Singapore, 1985) p. 723.
19. C. KITTEL, "Introduction to Solid State Physics" (Wiley, New York, 1967) Ch. 3 and 7.

Received 28 June
and accepted 21 December 1995